

An EXAFS Study of the Local Structure of the $\text{Pb}_{1-x}\text{Sn}_{1-x}\text{S}$ Solid Solution

A. I. Lebedev*, I. A. Sluchinskaya*, and I. H. Munro**

*Moscow State University, Vorob'evy gory, Moscow, 119899 Russia

e-mail: swan@mch.chem.msu.ru

**Daresbury Laboratory, Warrington, WA4 4AD U.K.

Received November 20, 2001

Abstract—The local lead-atom environment in the $\text{Pb}_x\text{Sn}_{1-x}\text{S}$ solid solutions with cubic and orthorhombic structure was studied by EXAFS spectroscopy. The shortest Pb–S distance in samples with orthorhombic structure was found to be smaller by ≈ 0.2 Å than that in cubic-lattice samples, which is a sign of stereochemical activity of the two paired $6s^2$ electrons of a Pb atom. The metal atom arrangement reveals strong short-range order, which results in the formation of –Pb–Sn–Pb–Sn–... zigzag chains aligned with the c axis (in the $Pbnm$ system) in orthorhombic samples. It was shown that the onset of such short-range order in $\text{Pb}_{0.5}\text{Sn}_{0.5}\text{S}$ can initiate the formation of superstructures belonging to the C_{2v}^2 or C_{2v}^7 space groups. © 2002 MAIK “Nauka/Interperiodica”.

1. INTRODUCTION

One of the problems encountered in studies of solid solutions is establishment of the relation between a deviation of a solid solution from its ideal structure and its physical properties.

The available scarce information on solid solutions in the SnS–PbS system is fairly contradictory. This system forms a limited number of solid solutions, because SnS has an orthorhombic structure (space group D_{2h}^{16} – $Pbnm$), while PbS has an NaCl-type cubic structure. The limiting solubility of SnS in PbS is ~ 10 mol %, and that of PbS in SnS is about 50 mol % [1–3]. There is no consensus on whether the $\text{Pb}_{0.5}\text{Sn}_{0.5}\text{S}$ composition (existing in nature in the mineral form of teallite [4]) in this system is an individual phase or a SnS-based solid solution. Some authors consider this composition to be an individual phase crystallizing in space group D_{2h}^{16} [2, 5, 6] or space groups D_{2h}^{13} or C_{2v}^7 [2, 6]. Others believe this material to be an SnS-based solid solution [1, 3, 7, 8]. To resolve this contradiction, coordinated studies of the short- and long-range order in samples of this composition are needed.

Our interest in the SnS–PbS system is connected with the off-centering of large-radius impurity ions, which was revealed earlier in the $\text{Ge}_{1-x}\text{Pb}_x\text{Te}$ and $\text{Ge}_{1-x}\text{Sn}_x\text{Te}$ semiconducting solid solutions [9]. The displacement of Pb and Sn atoms in these compounds to off-center positions was explained as being due to a deformation of the spherically symmetric electron-density distribution of the two paired s^2 electrons in these atoms. Being energetically favorable, this deformation

produced chemical bonds of unequal length. In what concerns Pb atoms, this came as a surprise, because the $6s^2$ lone pair in compounds of divalent lead is typically stereochemically inactive, as a result of which the local Pb environment in crystals is usually symmetric (as in PbS). It appeared, therefore, of interest to see whether the local environment of Pb atoms in SnS is distorted and whether it is associated with the stereochemical activity of their $6s^2$ electron pairs. In addressing this problem, we chose EXAFS spectroscopy. This modern x-ray method for investigating local structure is widely used in studies of the structure of solid solutions.

2. EXPERIMENTAL TECHNIQUE

2.1. Samples

Samples of the $\text{Pb}_x\text{Sn}_{1-x}\text{S}$ solid solution with $x = 0.1, 0.2, 0.35, 0.5,$ and 0.95 were prepared by synthesizing PbS and SnS and melting them in evacuated quartz ampoules, with subsequent annealing of the alloys at 645°C for 70–96 h. The phase homogeneity of the samples was checked by x-ray diffraction. At 300 K, the crystal structure of the samples with $x \leq 0.5$ corresponded to the orthorhombic phase and the structure of the $x = 0.95$ sample was cubic. Immediately before EXAFS spectral measurements, the alloys were ground to powder, sieved, and deposited on adhesive tape. The optimum absorber thickness for spectral measurements was obtained by repeatedly folding the tape.

The EXAFS spectra were obtained at the Pb L_{III} absorption edge (13.055 keV) at 80 K in transmission geometry on station 7.1 at the Daresbury Laboratory (Great Britain). The radiation was made monochro-

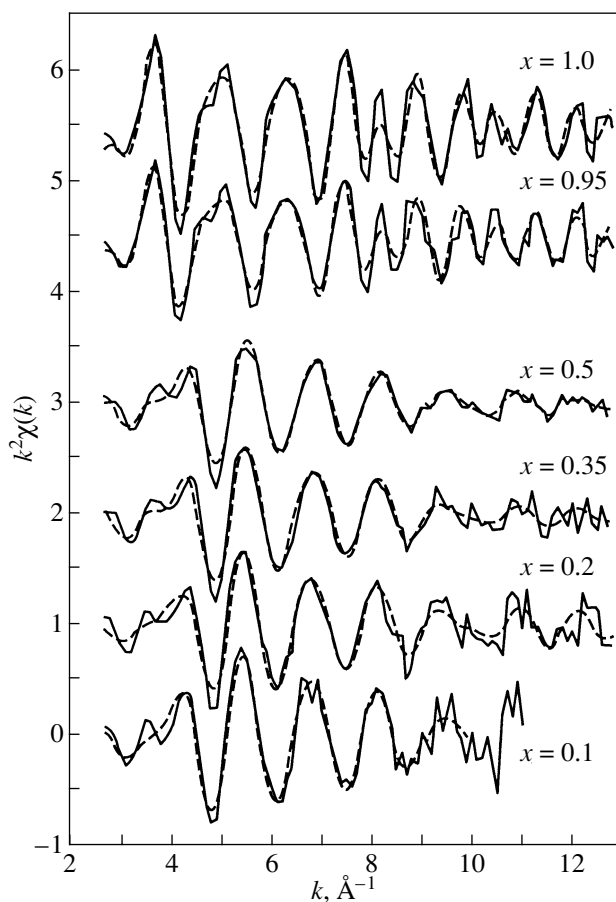


Fig. 1. Typical Pb L_{III} EXAFS spectra of lead obtained for $Pb_xSn_{x-1}S$ samples (solid lines) and their theoretical approximation (dashed lines).

matic by using a Si(111) double-crystal monochromator, and the intensity of the radiation incident on and transmitted through a sample was measured with ionization chambers. Two spectra were recorded for each sample.

2.2. Processing Technique

The EXAFS function $\chi(k)$ was extracted from $\mu_x(E)$ transmission spectra as was done in [10]. After subtraction of the background caused by the absorption of radiation by atoms other than Pb, the monotonic part of atomic absorption $\mu_{x_0}(E)$ was isolated by spline fitting and the dependence of $\chi = (\mu_x - \mu_{x_0})/\mu_{x_0}$ on wave vector $k = \sqrt{2m(E - E_0)}/\hbar$ was calculated. The photoelectron energy E_0 was reckoned from the inflection point at the absorption edge. The jump at the absorption edge varied from 0.10 to 1.5.

The information on the first three coordination shells of interest to us here was extracted by taking direct and inverse Fourier transforms of the $\chi(k)$ curves thus obtained using a modified Hanning window. The

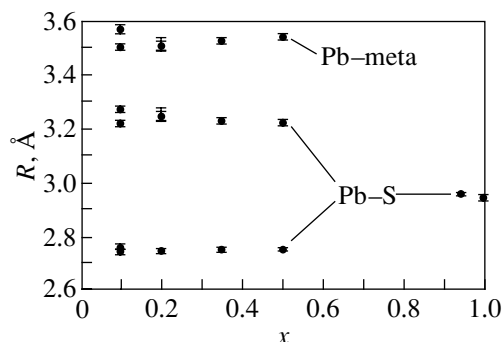


Fig. 2. Interatomic distances for the three nearest coordination shells of Pb atoms in the $Pb_xSn_{x-1}S$ solid solution plotted vs. composition parameter x .

range of isolation in the R space was typically 1.2–3.7 Å. The R_j distances, the coordination numbers N_j and the Debye–Waller factor σ_j^2 for each of the three coordination shells ($j = 1-3$) were derived by minimizing the rms deviation between the experimental and calculated $k^2\chi(k)$ curves. The parameters R_j , N_j , and σ_j^2 , as well as the origin displacement along the energy axis dE_0 , were varied. To reduce the number of variable parameters, the known relations between the coordination numbers in the SnS and NaCl structures were taken into account. The number of variable parameters (eight) was about two times smaller than that of independent parameters (15 or 16) in the $2\Delta R\Delta k/\pi$ data. The errors in determination of the parameters reported in the paper were found from the covariance matrix and correspond to a 95% confidence interval of their variation.

The dependences of the backscattering amplitude and phase, of the central-atom phase, and of the photoelectron mean free path on k , which are necessary to construct theoretical $\chi(k)$ curves, were calculated using the FEFF code [11].

3. EXPERIMENTAL RESULTS

Figure 1 shows typical $k^2\chi(k)$ relations obtained for all $Pb_xSn_{x-1}S$ samples. The curves for samples with cubic ($x \geq 0.95$) and orthorhombic ($x \leq 0.5$) structure differ qualitatively in pattern, which indicates different characters of the local Pb environment in these samples. An analysis of the data reveals that lead atoms in the $x = 0.95$ solid solution and PbS are surrounded by six sulfur atoms located at the same distance (see table and Fig. 2). The spectra obtained for samples with orthorhombic structure are described well only by the model according to which, in the first coordination shell, three S atoms sit at one distance from the central atom (R_1) and the other three sit at another distance (R_2). Thus, the nearest neighbor environment of Pb in SnS differs from that in PbS. As follows from the table, as x increases from 0.1 to 0.5, distance R_1 remains

Local Pb environment parameters for $\text{Pb}_x\text{Sn}_{1-x}\text{S}$ samples

Parameter	x						SnS*
	0.1	0.2	0.35	0.5	0.95	1	
$R_1, \text{\AA}$	2.750(8)	2.745(8)	2.752(4)	2.752(4)	2.954(8)	2.942(6)	2.660(3)
$\sigma_1^2, \text{\AA}^2$	0.0066(13)	0.0053(10)	0.0087(6)	0.0079(6)	0.0095(11)	0.086(9)	0.0036(4)
$R_2, \text{\AA}$	3.246(16)	3.243(16)	3.233(7)	3.232(8)	4.175(7)	4.184(6)	3.301(8)
$\sigma_2^2, \text{\AA}^2$	0.0174(35)	0.0120(26)	0.0178(14)	0.0187(16)	0.0064(7)	0.0066(6)	0.0059(8)
$R_3, \text{\AA}$	3.534(13)	3.500(15)	3.522(7)	3.535(10)			3.481(7)
$\sigma_3^2, \text{\AA}^2$	0.0081(16)	0.0090(15)	0.0118(8)	0.0141(12)			0.0067(6)

Note: The EXAFS data for the local environment of an Sn atom in SnS were obtained at the Sn K edge.

unchanged to within experimental error, whereas R_2 decreases slightly. Note also the fairly large value of the Debye–Waller factors for the longer Pb–S bond length.

In samples with orthorhombic structure, the metal atoms (Pb, Sn) in the second coordination shell are located at an average distance $R_3 \approx 3.5 \text{\AA}$, which grows insignificantly with x . The Debye–Waller factors for this shell (σ_3^2) turn out to be even smaller than (σ_2^2) (see table); however, their values grow noticeably with x .

As seen from the table, the Debye–Waller factors are the largest for the longer Pb–S bond length and depend only weakly on composition. To separate the contributions from thermal motion and static lattice distortions to the Debye–Waller factors, we measured the temperature dependences of EXAFS spectra for the $\text{Pb}_{0.8}\text{Sn}_{0.2}\text{S}$ sample within the temperature interval 80–300 K. An analysis of the data obtained showed that the temperature dependence of the Debye–Waller factor (σ_2^2) is stronger. One may thus conclude that the main contribution to (σ_2^2) is due not to static lattice distortions but rather to thermal vibrations. This suggests that the corresponding chemical bonding is weak.

Because solid solutions often exhibit short-range order, we decided to check whether this order is reflected in the metal atom arrangement in the second coordination shell. To check this possibility, we compared the experimental EXAFS spectra with the curves calculated for various ratios of Pb and Sn concentrations in the second coordination shell of lead under the assumption that the values of R_3 and (σ_3^2) for atoms of both types are equal. Figure 3 plots the sum of the squares of deviations, S_{\min} , for all the measured spectra as a function of the local Sn atom concentration in the second coordination shell of Pb atoms. We readily see that the minimum in the curves for samples with $x = 0.2, 0.35,$ and 0.5 lies at a local Sn concentration considerably in excess of its average concentration in the

sample; the local concentration averaged over several spectra for each of the samples studied is close to 100%. In our opinion, the short-range order in which Pb atoms are surrounded predominantly by atoms of Sn may be accounted for by the deformation interaction between metal atoms, which precludes two large-radius lead atoms from sitting close to one another.

4. DISCUSSION OF RESULTS

According to the neutron diffraction data available for SnS [12], six S atoms in the first coordination shell of tin lie at four different distances: 2.627 \AA (one atom), 2.665 \AA (two atoms), 3.290 \AA (two atoms), and 3.388 \AA (one atom). The two shortest distances are so close to each other that their separation in EXAFS spectra is impossible. The same applies to the two longest distances. For this reason, the nearest environment of

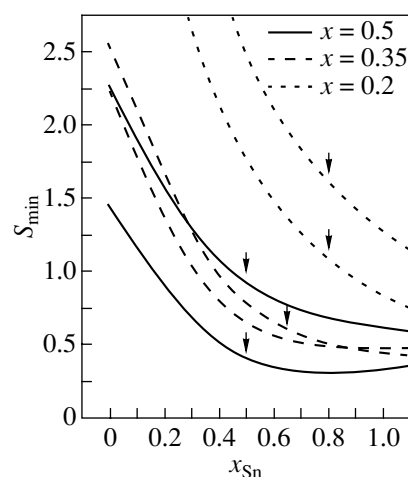


Fig. 3. Sum of the squares of deviations plotted vs. local Sn concentration in the second coordination shell of Pb atoms. Curves of one type belong to two spectra measured on samples of the same composition. Arrows identify the average Sn concentration in a sample.

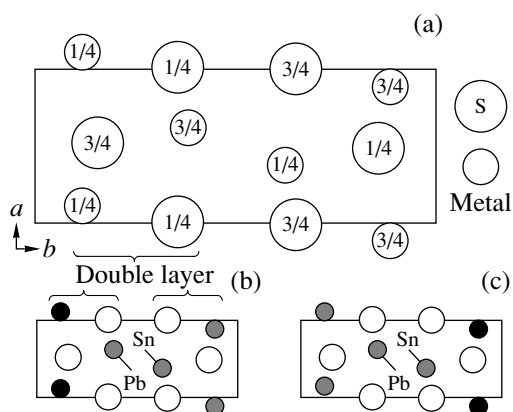


Fig. 4. (a) Projection of the SnS structure on the ab plane, and (b, c) two possible schemes of superstructural ordering of metal atoms in the $Pb_{0.5}Sn_{0.5}S$ solid solution. The space groups of the superstructures are (b) C_{2v}^7 and (c) C_{2v}^2 .

metal atoms in EXAFS spectra should be represented by three short and three long distances, each of them being determined by the averaged length of the constituent bonds. It is this that is observed experimentally.

As follows from a comparison of EXAFS data obtained for the local environment of Pb impurity atoms in SnS with those available for Sn atoms in pure SnS (see table), the shorter Pb–S bond length turns out to be ≈ 0.1 Å longer than the corresponding Sn–S bond length in SnS and the longer Pb–S bond length is shorter by ≈ 0.07 Å than the corresponding Sn–S distance in SnS.

Another result, which we believe to be most important, is that the short Pb–S bond length in samples with orthorhombic structure turned out to be noticeably shorter (by ≈ 0.2 Å) than that in PbS (2.94 Å). The decrease in this bond length and the splitting of the first coordination shell into two components indicate that Pb atoms in SnS occupy off-center positions. A comparison of our data with the results obtained in the study of the $Ge_{1-x}Pb_xTe$ solid solution [9] shows that, in both systems, the Pb–chalcogen bond lengths become different, with the decrease in the short bond length being nearly equal in both systems (≈ 0.2 Å). Significantly, the decrease in the Pb–chalcogen bond length is considerably smaller than the difference between the ionic radii of Pb^{2+} and Pb^{4+} (0.5 Å). This suggests that the two paired $6s^2$ electrons are not involved in chemical bonding, and we have here only a deformation in the density distribution of these paired electrons, i.e., a crossover to a stereochemically active state. In view of the fact that Pb is observed in off-center positions in SnS and GeTe, whereas introduction of Pb atoms into cubic SnTe does not entail, as we have seen, any local distortion of the symmetric environment, one can conclude that lead atoms become off-center only when they enter lattices with symmetry lower than cubic. Thus,

the density distribution of the paired $6s^2$ electrons of a Pb atom is mobile enough to be able to transfer from the inactive (as in PbS, PbSe, PbTe) to an active state under certain conditions. This feature of the paired lead electrons could account for the structural instability and phase transitions observed to occur in many lead compounds.

Our results also permit certain conclusions as to the structure of the solid solutions studied. According to our data, all the bond lengths in the nearest neighbor environment of Pb atoms in the $Pb_xSn_{x-1}S$ solid solution vary monotonically with x . This suggests that the $Pb_{0.5}Sn_{0.5}S$ composition in the SnS–PbS system should be considered to be an SnS-based solid solution.

Consider now the short-range order observed in this system. The SnS structure is known to consist of double-layer packets (Fig. 4a). The formation of a well-defined short-range order, in which Pb atoms in one double-layer packet are surrounded predominantly by Sn atoms of the neighboring packet, suggests that under certain conditions a superstructural metal-atom ordering observed in minerals (teallite) can set in $Pb_{0.5}Sn_{0.5}S$ crystals.

Assuming the local tin atom concentration in the second coordination shell of lead atoms to be 100%, we may expect that completely ordered zigzag chains $\dots-Pb-Sn-Pb-Sn-\dots$ aligned with the c axis (perpendicular to the plane of Fig. 4a) will form in $Pb_{0.5}Sn_{0.5}S$ samples. However, even if atoms in one such chain are fully ordered, three-dimensional long-range order (superstructure) can form only in the case where the atomic arrangements in neighboring chains are correlated. We note that the formation of zigzag chains destroys the inversion center in the crystal, which in the SnS structure lies midway between the two nearest neighbor tin atoms. This means that the space group of the superstructure must be a subgroup of space group D_{2h}^{16} and contain point group C_{2v} as a subgroup. Restricting oneself to analysis of superstructures without any change in unit-cell volume, two types of atomic ordering in the superstructure can be conceived: (1) one packet contains atoms of one species (space group $C_{2v}^7-P2_1nm$, Fig. 4b), and (2) one packet contains atoms of both species (space group $C_{2v}^2-Pb2_1$, Fig. 4c). Superstructures of the first type allow $(00l)$ superstructure reflections with odd l , while superstructures of the second type allow $(00l)$ and $(l00)$ reflections with odd l .

Electron diffraction patterns of thin $Pb_{0.5}Sn_{0.5}S$ films grown on substrates of alkali halide crystals at 200°C [8] exhibited reflections characteristic of a C_{2v}^2 superstructure. In an attempt to reproduce this result, we annealed a volume $Pb_{0.5}Sn_{0.5}S$ sample at 240°C for a month. X-ray studies of the annealed sample did not reveal any superstructural reflections. In our opinion, this may be due to the fact that the coupling energy of

neighboring chains (in which the shortest interatomic distance is ≈ 4.1 Å) is too low; therefore, annealing at lower temperatures is required. Thus, well-defined short-range order and the absence of long-range order in our samples indicates that interlayer coupling between metal atoms in the SnS-based solid solution under study is stronger than the intralayer coupling. This is in accord with the relative magnitude of the corresponding bond lengths (3.5, 4.1 Å).

Thus, the strong short-range order manifesting itself in the distribution of metal atoms permits one to consider the structure of the SnS–PbS solid solution to be in the form of randomly arranged fragments of zigzag chains aligned with the *c* axis of the structure. The clearly pronounced anisotropy of the local structure may account for the unusual physical properties of these solid solutions.

The short-range order in the arrangement of metal atoms is also directly reflected in the phase diagram of the SnS–PbS system. As already mentioned, the extent of the single-phase region in the phase diagram of the solid solution on the SnS side is $\approx 50\%$. Our analysis suggests that this concentration corresponds to the limiting case where all metal atoms are ordered in zigzag chains. At higher Pb atom concentrations, Pb–Pb pairs should inevitably appear in the chains, whose formation is energetically unfavorable. It is this factor that determines the boundary of existence of the solid solution in the system studied.

REFERENCES

1. I. S. Morozov and C.-F. Li, *Zh. Neorg. Khim.* **8** (7), 1688 (1963).
2. V. G. Kuznetsov and C.-F. Li, *Zh. Neorg. Khim.* **9** (5), 1201 (1964).
3. H. von Krebs and D. Langner, *Z. Anorg. Allg. Chem.* **334** (1–2), 37 (1964).
4. *Minerals: a Handbook* (Akad. Nauk SSSR, Moscow, 1960), Vol. 1, pp. 370–373.
5. T. Baak, E. D. Dietz, M. Shouf, and J. A. Walmsley, *J. Chem. Eng. Data* **11** (4), 587 (1966).
6. A. D. Bigvava, É. D. Kunchuliya, S. S. Moiseenko, and B. B. Anisimov, *Izv. Akad. Nauk SSSR, Neorg. Mater.* **10** (2), 539 (1974).
7. Z. M. Latypov, N. R. Faizullina, V. N. Savel'ev, and R. Yu. Davletshin, *Izv. Akad. Nauk SSSR, Neorg. Mater.* **12** (2), 206 (1976).
8. I. R. Nuriev, É. Yu. Salaev, and R. N. Nabiev, *Izv. Akad. Nauk SSSR, Neorg. Mater.* **22** (2), 204 (1986).
9. A. I. Lebedev, I. A. Sluchinskaya, V. N. Demin, and I. H. Munro, *Phys. Rev. B* **55** (22), 14770 (1997).
10. A. I. Lebedev, I. A. Sluchinskaya, V. N. Demin, and I. H. Munro, *Fiz. Tverd. Tela (St. Petersburg)* **41** (8), 1394 (1999) [*Phys. Solid State* **41**, 1275 (1999)].
11. J. Mustre de Leon, J. J. Rehr, S. I. Zabinsky, and R. C. Albers, *Phys. Rev. B* **44** (9), 4146 (1991).
12. T. Chattopadhyay, J. Pannetier, and H. G. von Schnering, *J. Phys. Chem. Solids* **47** (9), 879 (1986).

Translated by G. Skrebtsov

SPELL: meta